Journal of Biomedical Optics

BiomedicalOptics.SPIEDigitalLibrary.org

Extension of the concept of an anomalous water component to images of T-cell organelles

Vladimir P. Tychinsky

SPIE.

Extension of the concept of an anomalous water component to images of T-cell organelles

Vladimir P. Tychinsky
Moscow State Institute of Radioengineering, Electronics and Automation (TU), Laboratory of Coherent Optics, 78 Vernadsky Avenue, Moscow 119454, Russia

Abstract. Microscopic images of a living cell are the main source of information on its functional state. Modern interference microscopy techniques allow the numerical parameters of cell images to be obtained with an accuracy not available with other methods. Quantitative analysis of phase images of T lymphocytes (TCs) in different functional states demonstrated that variations of the properties of intracellular water should be taken into account. This conclusion agrees with the current view that the physical parameters of water, including the refractive index (RI) of a water layer, depend on the hydrophilicity and other characteristics of the adjacent surface. Application of this concept to phase images of TCs showed that the contribution of the fourth phase of water (4-water) or the structured water component, which has an increased RI, should be considered. The proportion of 4-water depends on the functional state of the cell determined by the culture medium composition. Normally, the proportion of 4-water in organelles is as high as 30%; it is considerably lower in organelles of cells with inhibited metabolism. [DOI: 10.1117/1.JBO.19.12.126008]

Keywords: coherent phase microscopy; subcellular structures; optical model of the living cell; T-lymphocyte; the fourth state of water.

Paper 140359R received Jun. 6, 2014; accepted for publication Oct. 27, 2014; published online Dec. 15, 2014.

1 Introduction

Water is one of the best studied environmental objects. Its properties are dealt with in a number of studies (reviewed in Ref. 1). Therefore, new data on structured water or the fourth phase of water (4-water) summarized and systematized in a recent book by Pollack[2] are of particular interest. The 4-water has a number of anomalous properties expressed in the so-called exclusion zones of water layers adjacent to hydrophilic surfaces and in gels. Two simple examples clearly illustrate these properties of 4-water. The refractive index (RI) of a gel containing 99% of water has been found to drastically decrease from $n = 1.43$ to $n_0 = 1.333$ (a value characteristic for ordinary water) upon heating by only 1°C.[3] The second example is an RI of a water $n \approx 1.43$ at the hydrophilic surface of Nafion, a synthetic polymer with ionic properties.[4,5,6]

Cells of most organisms contain as much as 80% of water; in jellyfish, the percentage exceeds 95%. Therefore, it is logical to assume that the component referred to as 4-water[2] somehow affects microscopic phase images of cells and is detectable in these objects.[7–11] However, we have not found any mention of such a phenomenon in the literature. This also applies to cell images obtained by various interference microscopy methods; no effect of 4-water on the images has been reported.[12–15]

Quantitative analysis of phase images of various cell types[7–12] has shown that the changes in their optical parameters caused by external factors cannot be solely explained by alterations of their proteins. In solving this problem, we suggested[7–12] that not only the change in protein RI averaged by the cell volume should be taken into account, but the possibility that the RI of intracellular water is changed should also be assumed. To test this hypothesis, we took advantage of the unique properties of cell phase images[16] and original algorithms.[10,11]

Here, we used RI measurements of T lymphocyte (TC) to calculate the proportion of the anomalous water component (4-water) in the organelles. To our knowledge, these are the first quantitative estimations of the mass fraction of 4-water in TC organelles. We present data on the 4-water effect on the organelle contrast in the phase image of a cell. For this purpose, we proposed a multicomponent optical model of a TC.

The basic assumption of our hypothesis is the existence of 4-water as a factor that contributes to RI. We also hypothesized that the proportions of 4-water and ordinary water in a living cell depended on its functional state.[6,7] Below, we provide a biophysical interpretation of the variation of the 4-water contribution to the RIs of organelles and an explanation of its dependence on the hydrophilic/hydrophobic properties of organelles' membranes. We believe that our results can be used for explaining other phenomena in cell biophysics.

2 Theory

2.1 *Optical Model: Concept of Zones and Characteristic Parameters in the Phase Image of the Cell*

Common for all interference methods is the representation of the images in the form of a two-dimensional distribution $h(x, y)$ of optical path difference (OPD) in the image plane. The most important and the unique advantage of the interference microscopy is the measurement of OPD in absolute units of wavelength[7–19] with a very high precision, which is hardly achievable or is even impossible with other methods. Normally, the phase image is described as the function

$$h(x, y) = \int (n(x, y, z) - n_0) \mathrm{d}z$$

Author Vladimir Tychinsky is deceased.

Address all correspondence to: Tatiana Vyshenskaya, E-mail: tvysh@yandex.ru

in the image plane (x, y), where $n(x, y, z)$ and n_0 are the refractive indices of the object and the environment, respectively. The function $h(x, y)$ can be interpreted as a "projection" of the refractive index onto the image plane. Under certain conditions, the inverse problem can be solved when the function $h(x, y)$ is restored from its projection.

We also used an optical model of TC.[11] Its structure was represented by a limited number of spherical layers with different RIs (n_i) or refractivities $\Delta n_i = n_i - n_0$. In the phase image $h(x, y)$, these layers were projected onto the plain (x, y) as zones outlined with the contours $h_{ij}(x, y) = \text{const}$ (Fig. 1). We have previously shown the possibility of determining the physical parameters of structural elements at the boundaries of these zones[10,11] as a system of concentric spherical layers with the diameters d_{ij} and volumes $V_{ij} = \pi(d_i^3 - d_j^3)/6$. In general, the value of OPD at the boundary of j, $j + 1$'th zones can be represented as the sum: $h_{j,j+1} = \sum H_{ji}\Delta n$, where $\Delta n_i = n_i - n_0$ is its refractivity; in the geometric path H_{ji}, the first index j corresponds to the position of the point, and the second index i corresponds to the number of the layer $(1 \le i \le j)$. The OPD "jumps" in the image plane (x, y) in the proximity of the points that are the projections of the adjacent layer due to the difference $(\Delta n_{j+1} - \Delta n_j)$.

A very high resolution of phase images is an important and a specific feature of phase images obtained as a raster series of pixels with a high precision.[16–19] The phase thickness (h_{ij}) at the boundaries of organelles[11] was determined from the coordinates of the characteristic points (CPs) of the integral functions of area:

$$S(h) = \int \mathrm{d}x\,\mathrm{d}y \tag{1}$$

and phase volume

$$W(h) = \int \Delta n(x, y, z)\mathrm{d}x\,\mathrm{d}y\,\mathrm{d}z. \tag{2}$$

These plots are shown in Figs. 1(c) and 1(d), respectively. The positions of the $S_{ij}(h_{ij})$ and $W_{ij}(h_{ij})$, the CPs and their abscissas on the plots were determined from the maxima of the derivatives dS/dh and dW/dh. This allowed us to exclude the minor nonuniqueness of the abscissas (h_{ij}) related to the asymmetry of cell shape and phase thickness profiles in Fig. 1(a). The following equation was used to determine the "equivalent" symmetric half-profile $h(r)$ shown in Fig. 1(e):

$$S(h) = \pi r^2(h). \tag{3}$$

This made it possible to use the diameters of circles interpreted as the boundaries of zones [Fig. 1(a)]:

$$d_{ij} = 2\left(\frac{S_{ij}}{\pi}\right)^{\frac{1}{2}}. \tag{4}$$

Double indices (i and $j = i + 1$) were used to designate the phase thickness (h_{ij}) and other parameters of the CPs. For example, the index $ij = 01$ corresponded to the outer boundary of the cell and cytoplasm. The following main zones were distinguished: 0, environment (incubation medium); 1, peripheral cytoplasm; 2, its dense part (endoplasmic reticulum); 3, nucleus; and 4, nucleoli.

One can hypothesize that each organelle can be represented as a multicomponent spherical layer in the TC optical model.

2.2 *Multicomponent Optical Model*

The ultimate goal of the study was to determine the proportion of 4-water in each layer at different functional states. For this purpose, we used the condition of additive contributions of components, which is well known from the physics of dielectrics. It consists in the presentation of the electrical (or optical) properties of a multicomponent medium as a sum of the electrical susceptibilities of its components:

$${}^{\Sigma}\chi_i = \sum \chi_i = {}^{\Sigma}n_i^2 - 1. \tag{5}$$

This is important since only susceptibility, but not RI, meets the condition of additive contributions of the components.

Here, we considered only two water and two protein components designated by double left subscripts (11 and 12 for water and 22 and 21 for protein). The subscripts for ordinary water and protein components are 11 and 22, respectively; those for anomalous components are 12 and 21, respectively. Component 12 is the aforementioned susceptibility of water molecules (4-water), e.g., in layers adjacent to the hydrophilic areas of membranes. Correspondingly, component 21 is the expected change in the susceptibility of protein molecules (4-protein). The notations used here for the proportions of components $({}^0_{11}\eta$ and ${}^0_{22}\eta)$, where the obvious condition ${}^0_{11}\eta + {}^0_{22}\eta = 1$ should be met in an ideal medium (in the absence of anomalous components). The zero left superscript in ${}^0_{ii}\eta$ indicates the ideal medium. The summary susceptibility of this ideal binary medium $({}^0_{\Sigma}\chi)$ with the proportions ${}^0_{11}\eta$ and ${}^0_{22}\eta$ and susceptibilities ${}^0_{11}\chi$ and ${}^0_{22}\chi$ can be calculated as

$$\begin{aligned} {}^0_{\Sigma}\chi &= {}^0_{11}\chi{}^0_{11}\eta + {}^0_{22}\chi{}^0_{22}\eta = {}^0_{11}\chi + {}^0_{22}\eta({}^0_{22}\chi - {}^0_{11}\chi) \\ &= {}^0_{22}\chi + {}^0_{11}\eta({}^0_{11}\chi - {}^0_{22}\chi). \end{aligned} \tag{6}$$

For the known susceptibilities of the main components, ordinary water and protein $({}^0_{11}\chi$ and ${}^0_{22}\chi$, respectively), it depends only on their weight proportions. Correspondingly, the total susceptibility of the four-component medium (including the anomalous water and protein components) is represented in the form of the equation

$${}_{\Sigma}\chi_i = {}_{11}\chi_{i11}\eta_i + {}_{12}\chi_{i12}\eta_i + {}_{21}\chi_{i21}\eta_i + {}_{22}\chi_{i22}\eta_i \tag{7}$$

or as the ${}_{\Sigma}\chi_i = \sum_{kl} {}_{kl}\eta_{ikl}\chi_i$, where summation is performed over the indices of organelles (i) and their components $(kl = 1, 2)$ determining the susceptibility of each i'th layer. The normalization condition for the weight proportions of all components $({}_{kl}\eta_i)$ has the standard form $\sum_{kl} {}_{kl}\eta_i = 1$.

Our third hypothesis is that the susceptibility of the medium of the i'th organelle and the parameters of the organelles of a T cell in the functional state p can be represented by the refractive and susceptibility indices of each i'th layer: $({}^p n_i)^2 = 1 + {}^p\chi_i$. In these notations, the change in the susceptibility of the i'th organelle medium upon transition of the T cell from states p to q is

$${}^{pq}\chi_i = {}^p\chi_i - {}^q\chi_i = \sum_{kl} {}^p_{kl}\eta_i{}^p_{kl}\chi_i - \sum_{kl} {}^q_{kl}\eta_i{}^q_{kl}\chi_i. \tag{8}$$

Within the correctness of the aforementioned three hypotheses, the refractivity and susceptibility profiles based on measurements of a TC can be used to quantitatively estimate the

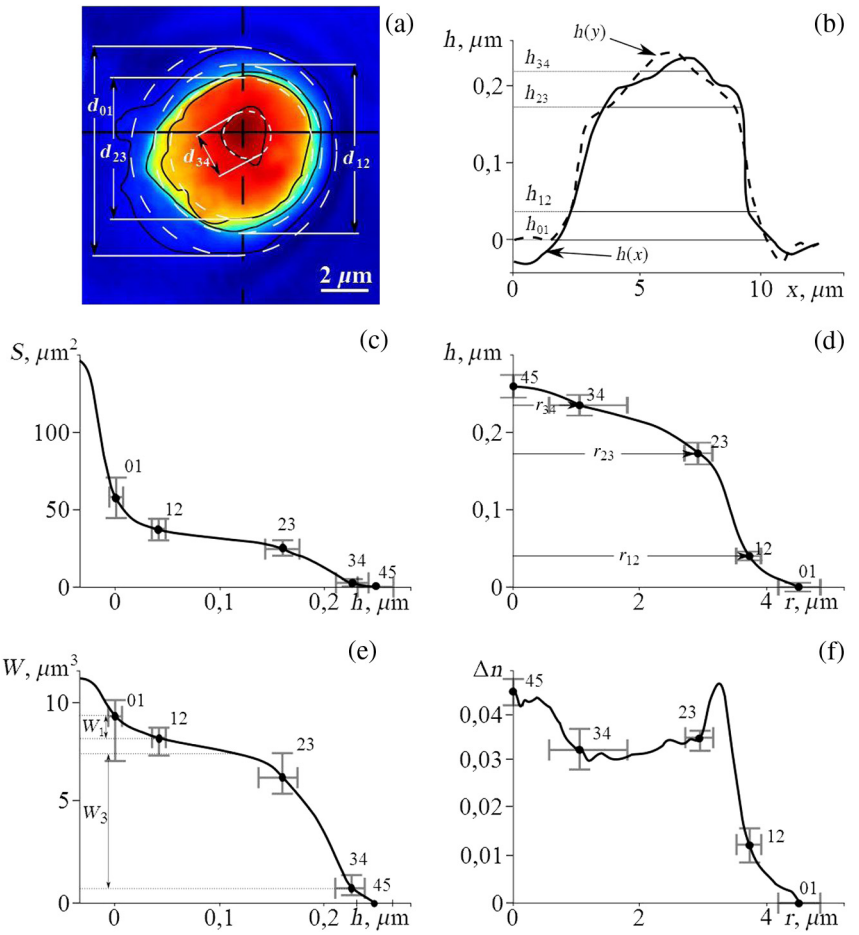

Fig. 1 Physical basis of the concept of significant parameters of phase images. Algorithms and other tools used for phase image analysis. (a) A phase image $h(x, y)$ of a T lymphocyte (TC) obtained using an interference microscope as a two-dimensional distribution of the optical path difference in the plane (x, y). Structural elements differ from one another in the refractive index; their boundaries are shown as the contours $h_{ij}(x, y) = \text{const}$. Dotted circles d_{ij} have the same areas (S_{ij}) as those outlined with the contours h_{ij}. Zones (1 to 4) represent TC organelles. (b) Phase thickness profiles $h(x)$ and $h(y)$ (dotted line) in diametric sections of a TC image. The values h_{ij} ($j = i + 1$) correspond to the boundaries between structural elements: 01, the external medium and the peripheral cytoplasm; 12, the cytoplasm and the endoplasmic reticulum; 23, the endoplasmic reticulum and the nucleus; 34, the nucleus and the nucleolus. (c) The plot of the integral function of the area $S(h)$. Characteristic points with coordinates $[S_{ij}, h_{ij}]$ where the derivative dS/dh has maxima are shown. The h_{ij} values correspond to the positions of boundaries in Figs. 1(a) and 1(b). (d) The $h(r)$ plot interpreted as a centrally symmetric equivalent of the real profiles $h(x)$ and $h(y)$ of the TC phase thickness in the normal state. The radius of the circle at the boundary of organelles in Fig. 1(a) (r_{ij}) is determined from the area $S_{ij} = \pi r_{ij}^2$, $S_{ij} = \pi(r_{ij})^2$ in the ij'th characteristic point in Fig. 1(c). (e) The integral function $W(h)$ of the phase volume reflects the optical heterogeneity of the TC. The peripheral cytoplasm makes a contribution to the phase volume of zone 1 ($W_1 = W_{01} - W_{12}$) limited by the radii r_{01} and r_{12}. The largest contribution to the phase volume of zone 3 is made by the nucleus. The W_{ij} values are related to the organelle refractivities and are important parameters of the phase portrait of the cell. These images have been obtained using the raster scanning method.[16–19] (f) The refractivity profile $\Delta n(r)$ of the TC in the normal state. The low $\Delta n^1(r) \leq 0.01$ between r_{01} and r_{12} in the region of zone 1 corresponds to the peripheral cytoplasm. A considerable increase in refractivity has been observed in the optically dense endoplasmic reticulum region (zone 2) in the normal state. The nucleus (zone 3) accounts for the largest part of the cell volume with a somewhat lower optical density [$\Delta n^3(r) \approx 0.032 - 0.035$]. The local increase in refractivity $\delta n^{45} = \Delta n^{45} - \Delta n^{34} \approx 0.01$ in the center of the cell corresponds to a higher density of the nucleolus. Twenty cells were measured in each media.

changes in the proportions of the components of their medium. In particular, this method allows the proportion of the anomalous water component (4-water) in organelles to be determined and used for biophysical interpretation.

We represented the functional state of a TC as its phase portrait, with "primary" parameters in the zones and their values of $S_{ij}(h_{ij})$ and $W_{ij}(h_{ij})$ at the boundaries. These parameters are universal because their estimates in the phase image of the cell are independent of its type and the optical model used. It has been demonstrated that, in the context of the aforementioned three hypotheses, the RIs of organelles found from the measurements can be used to quantitatively estimate the parameters of

their medium. In particular, the proportions of the anomalous water component (4-water) in organelles have been determined and used for biophysical interpretation. The change in the proportion of 4-water $({}^{p}_{12}\eta_i - {}^{q}_{12}\eta_i)$ can be estimated from the values of $({}^{p}_{11}\chi_i - {}^{p}_{12}\chi_i)$ known *a priori* and the results of the measurement of organelle refractivities ($\Delta^p n_i$ and $\Delta^q n_i$) as

$$\Delta^{pq}_{1}\chi_i = ({}^{p}_{11}\chi_i - {}^{p}_{12}\chi_i)({}^{p}_{12}\eta_i - {}^{q}_{12}\eta_i)$$
$$= (\Delta^p n_i - \Delta^q n_i)(2_0 n + \Delta^p n_i + \Delta^q n_i). \quad (9)$$

3 Materials and Methods

TCs isolated from the blood of a healthy donor were in the G0 phase. Details of the technique and specimen preparation have been described earlier.[8–11] The functional state of TCs was changed by the addition of compounds with a known mechanism of pharmacological action. We used the concentrations of compounds generally reported in the literature for treatment of whole cells and organelles. Media are designated as follows: N, phosphate buffer saline (PBS); P, R, and F, PBS supplemented with 2 μg/ml prednisolone, 1 μM rotenone, and 4% formalin, respectively. We also exposed TCs to controlled He–Ne laser radiation ($\lambda = 633$ nm, 1 mW) with a light dose of 10^5 J/m^2. This laser was used as a source in the Airyscan coherent phase microscope for phase imaging of cells. The cells were placed into a cuvette under a cover slip, then the cuvette was fixed on a microscope stage.

Phase images $h(x, y)$ of TCs in different incubation media were obtained using an Airyscan coherent phase microscope.[8–11] All experiments were performed with the Olympus MD Plan 20* objective, NA 0.4. The raster method of image recording was used in contrast to the studies that employed the multistep method.[12–15] New physical parameters of TC organelles (the phase volume, exclusion zone areas, phase thickness, and RIs profiles) were obtained using our originally developed algorithms.[10,11]

4 Results

The proposed approach is illustrated by TC images obtained with the Airyscan coherent phase microscope.[11] Irradiation for as long as 40 min caused changes in the cells, expressed most distinctly in a decreased contrast of CPs in the plots of integral functions[10] and a decreased phase thickness. Earlier we have demonstrated that the decrease of phase height of the isolated mitochondria and chloroplasts is proportional to the drop of the transmembrane potential.[8,9] This state designated D was considered to correspond to a complete de-energization of cells (stopped metabolism). The refractivity profile $\Delta n(r)$ (Fig. 2) corresponds to this energetically lowest state. Hereafter, we refer to the coordinates of CPs and the parameters at the boundaries of organelles, with the organelles indicated by the following subscripts: 1, cytoplasm; 2, endoplasmic reticulum; 3, nucleus; 4, nucleolus. As seen in Fig. 2, the N, P, R, and F components of the medium had differential effects on the refractivity profile of organelles. Prednisolone caused a local decrease in refractivity in zones 4 (the nucleolus) and 2 (the endoplasmic reticulum). The effects of rotenone and formalin were characterized by a more monotonous and a significant decrease in refractivity toward the cell periphery (zones 2 and 1). Noteworthy is a decreased contrast of the intermediate CPs ($ij = 12$, 23 and 34) in the R and F refractivity profiles.[11]

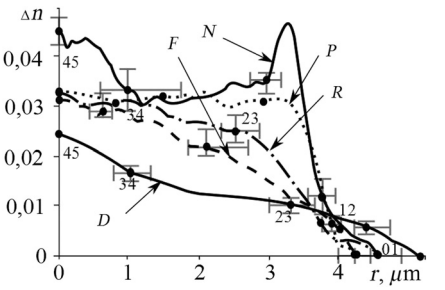

Fig. 2 Refractivity profiles of a TC in different media. The indices N, P, R, and F indicate the states of the cell in these media: N, physiological phosphate buffer saline (PBS; normal state); P, medium containing prednisolone; R, the medium containing rotenone; F, medium containing formalin; D, PBS, 40 min of laser irradiation. The differences between the responses of organelles are represented in the refractivity profiles. Points with double indices indicate the radii (r_{ij}) of the organelle boundaries. The smallest changes have been observed in the prednisolone-containing medium. The general decrease in refractivity attributable to de-energization is the most distinct in the endoplasmic reticulum region. Twenty cells were measured in each media.

The effects of the incubation medium and other environmental factors on the functional state of TCs have been previously analyzed. It is known that rotenone blocks the complex 1 of the respiratory chain, and formalin inhibits metabolic processes. Manteifel and Karu[20] have studied the effect of laser radiation on TCs in detail and obtained electron microscopic images of irreversible changes in the cell structural elements.[20]

The main goal of our study was quantitative estimation of the effect of 4-water and changes in its proportions in cell organelles $\Delta^{pq}_{12}\eta_i$ on the parameters of TC phase images. The estimation was based on the refractivity profiles $\Delta n(r)$ shown in Fig. 2 and Eqs. (6) and (7) at ${}_{12}n = 1.43$ (${}_{12}\chi = 1.05$) for the RI of the anomalous 4-water component.[8–10] For the anomalous protein component, we assumed ${}_{21}n \approx 1.4$ (at a susceptibility of ${}_{21}\chi = 1$), the mean protein susceptibility being assumed to be ${}_{22}\chi = 1.2$ (${}_{22}n = 1.44$). These values corresponded to a difference of susceptibilities of ${}_{12}\chi - {}_{11}\chi = 0.273$.

Figure 3 shows the calculated profiles of changes in the proportions of 4-water $\Delta^{pq}_{12}\eta_i(r)$ in different media. Note that the change $\Delta^{ND}_{12}\eta_i(r)$ upon transition from the normal state into the de-energized one (ND) was the largest. The maximum changes were observed in the endoplasmic reticulum zone ($i = 2$, $\Delta^{ND}_{12}\eta_2 \approx 40\%$) at a distance of $r \approx 3.2$ μm from the nucleolar zone ($i = 4$, $\Delta^{ND}_{12}\eta_4 \approx 20\%$). In the nuclear zone ($r = 1.5$ to 2.0 μm), the decrease in the 4-water share was smaller ($\Delta^{ND}_{12}\eta_3 \approx 10\%$); in the peripheral cytoplasm, it was almost indistinguishable ($\Delta^{ND}_{12}\eta_1 \approx 3\%$). As expected, the changes upon transitions

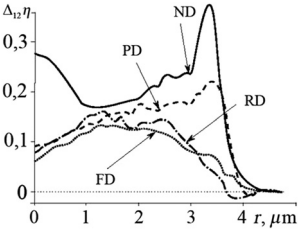

Fig. 3 Changes in the proportion of fourth phase of water (4-water) $\Delta^4\eta(r)$ upon the transitions from N, R, P, and F states of TC (see Fig. 2) to fully de-energized D state (ND, RD, PD, and FD transitions). The largest changes have been observed in the endoplasmic reticulum (zone 2) and the nucleolus (zone 4).

from the R and P states into the D state ($\Delta_{12}^{RD}\eta(r)$ and $\Delta_{12}^{PD}\eta(r)$, respectively) were smaller. Noticeable changes in the proportions of 4-water occurred only at the periphery of the nucleus and in the endoplasmic reticulum zone, and only in the cells incubated in the prednisolone containing medium. The changes were detected only in the region of the maximum refractivity [point $\Delta_{12}^{ND}\eta_2(r=3.2)$].

Interpreting the results shown in Fig. 3, we used the refractivity profile of the whole cell (Δn_i). Equation (6) was used for quantitative estimation of the changes in the proportions of the components for protein and water. The ratio between the complete protein and water amounts was taken as ${}_2\eta_i/{}_1\eta_i = 1/4$ according to the assumed constant 80% water content of the cell.

We also performed estimations for an alternative model of a cell, where the constant contribution of the protein component (20%) to the cell image was ignored. As expected, the changes in the refractivity ($\Delta^p n_i - \Delta^q n_i$) and susceptibility of water (${}_1^{pq}\chi_i$) were increased by ${}_2\eta_i/{}_1\eta_i = 1/4 = 25\%$.

For an alternative and unrealistic case of an "equivalent" cell with the constant parameters of ordinary water ($\Delta^p n_i = \Delta^q n_i = 1.333 = \text{const}$), the changes should be attributed to the protein component alone. This leads to the conclusion that the changes in the protein refractivity and susceptibility should be four times higher (${}_1\eta_i/{}_2\eta_i = 4$) than those indicated above for the variable water component. In such an "equivalent" cell, the ratio of refractivities $\Delta^p n_i$ and $\Delta^q n_i$ in organelles upon pq transition would be two times higher: $({}_{22}\eta_i/{}_{21}\eta_i)^{1/2} = 2$. Obviously, these changes cannot be explained by any reasonable assumption.

As seen in Fig. 2, the changes in refractivity are the largest upon ND transition in the endoplasmic reticulum zone ($i = 2$), where the difference reached $\Delta^N n_2 - \Delta^D n_2 \approx 0.025$.

Therefore, even if we take the 25% underestimation of the 4-water RI that results from neglecting the contribution of the protein into account, we obtain reasonable values of the change in refractivity ($n_{21} = n_0 - \Delta^N n_{21} = 1.37$) or the values $\Delta^N n_3 - \Delta^D n_3 \approx 0.037$ upon ND transition at a protein proportion of ${}_2\eta = 0.2$. This corresponds to changes in susceptibility of $\Delta^{ND}\chi_3(3) \approx 0.051$ and $\Delta^{ND}\chi_3(2.5) \approx 0.034$.

In an alternative model, it should be assumed that the minimum RI of the nucleus in the completely de-energized state always remains within the interval ${}^D n_3 \approx 1.38 - 1.39$ (${}^D\chi_3 \approx 0.9 - 0.93$). Hence, in the energized states, the nucleus RI should vary only within the interval ${}^N n_3 \approx 1.5 - 1.59$. Obviously, this result cannot be explained on the basis of known data.

Our analysis leads to the following preliminary conclusions:

1. The measured RI values in different metabolic states of a TC cannot be explained assuming an 80% water component with invariable standard physical parameters.
2. The only feasible explanation is the assumption of variable parameters for water.

5 Discussion

This study considers a number of debated issues. The main one is the hypothesis of the existence of 4-water in a living cell. Monographs by Ling[21] and Pollack[2] were apparently the first to discuss the problem of a structured water component in cells. However, only the experimental finding of exclusion zones in water layers adjacent to hydrophilic surfaces made it possible to discuss the issue in terms of modern physics.[6] The first and very important finding was the existence of 4-water with a higher RI compared to ordinary water. Hence, it is possible to detect 4-water by interference methods.[4–7] Unfortunately, judging from the available literature, this fact has not been addressed at the level it deserves.

Measurements of RIs (or refractivity) of organelles of living cells, in particular, TCs,[11] constituted the next step of research. We believe that this step was of no less importance for cell biophysics, because the use of cell volume averaged RI was insufficient for calculating the contribution of the anomalous 4-water component.

The available literature does not contain any discussion of the problem considered here, including that of 4-water in living cells. We were the first to use the numerical analysis of the dependence of refractivity values on electric susceptibility for determination of the cell organelle response to external factors, including the incubation media.[7] There are grounds to believe that the concept of 4-water can be extended to other cell types, and new algorithms can be developed to quantitatively estimate this parameter. Evidently, similar results can be obtained for various cells using other types of interference microscopes.

6 Concluding Remarks

In this study, we considered only two water components (indices 11 and 12) and two protein components (indices 22 and 21). Component 12 reflects the expected change in the contribution to the susceptibility of water (4-water) molecules in layers adjacent to hydrophilic areas of membranes. Correspondingly, component 21 should reflect a similar change in the susceptibility of protein (4-protein) molecules. We do not know a more primitive and a simple optical model of a cell that would allow the proportion of the anomalous water component to be estimated. Apparently, our third hypothesis that a cell (a TC, in the given case) can be considered as a multicomponent layered medium with $({}^p n_i)^2 = 1 + {}^p\chi_i$ does not contradict current views (see Sec. 2.2).

An important general conclusion is that the changes of the i'th organelle in the initial functional state p of a TC can be represented in terms of the contributions of different components of its susceptibility:

$$ {}^{pq}\chi_i = {}^p\chi_i - {}^q\chi_i = \sum_{kl}^{p} \eta_{ikl}^{p}\chi_i - \sum_{kl}^{q} \eta_{ikl}^{q}\chi_i. \tag{10} $$

Acknowledgments

This study was supported by the Russian Foundation for Basic Research (Grant No. 13-02-00278) and the Ministry of Education and Science of the Russian Federation. I am grateful to A. Shtil for critical discussions, T. Vyshenskaya for T cell measurements, V. Zverzhkhovsky for design of original algorithms, and V. Ushakov for help in manuscript preparation.

References

1. M. Chaplin, "Water structure and science," www.lsbu.ac.uk/water/water_structure_science.html (10 May 2014).
2. G. Pollack, *The Fourth Phase of Water*, Ebner & Sons Publishers, Seattle (2013).
3. B. W. Garner et al., "Refractive index change due to volume-phase transition in polyacrylamide gel for optoelectronics and photonics," *Appl. Phys. Express* **2**(5), 7001 (2009).
4. N. F. Bunkin et al., "Study of the phase states of water close to nafion interface," *Water* **4**, 129–154 (2013).

5. N. F. Bunkin et al., "Colloidal crystal formation at the 'nafion–water' interface," *J. Phys. Chem. B* **118**, 3372–3377 (2014).
6. V. Tychinsky, "High electric susceptibility is the signature of structured water in water-contained objects," *Water J.* **3**, 95–99 (2010).
7. V. Tychinsky, "The metabolic component of cellular refractivity and its importance for optical cytometry," *J. Biophotonics.* **2**(8–9), 494–504 (2009).
8. V. P. Tychinsky and A. N. Tikhonov, "Visualization of individual cells and energy-transducing organelles," *Cell Biochem. Biophys.* **58**(3), 117–128 (2010).
9. V. Tychinsky, A. Kretushev, and T. Vyshenskaya, "Mitochondria optical parameters are dependent on their energy state: a new electro-optical effect?," *Eur. Biophys. J.* **33**(8), 700–705 (2004).
10. V. P. Tychinsky et al., "Quantitative phase imaging of living cells: application of the phase volume and area functions to the analysis of 'nuclear stress'," *J. Biomed. Opt.* **18**(11), 111413 (2013).
11. V. P. Tychinsky et al., "Dissecting eukaryotic cells by coherent phase microscopy: a quantitative analysis of quiescent and activated T-lymphocytes," *J. Biomed. Opt.* **17**(7), 076020 (2012).
12. L. Wang et al., "Spatial light interference microscopy (SLIM)," *Opt. Express* **19**(2), 1016–1026 (2011).
13. B. Bhaduri, K. Tangella, and G. Popescu, "Fourier phase microscopy with white light," *Biomed. Opt. Express* **4**(8), 1434–1441 (2013).
14. B. Rappaz et al., "Measurement of the integral refractive index and dynamic cell morphometry of living cell with digital holographic microscopy," *Opt. Express* **13**, 9361–9373 (2005).
15. Y. Park et al., "Static and dynamic light scattering of healthy and malaria-parasite invaded red blood cells," *Proc. Natl. Acad. Sci. U. S. A.* **105**, 13730 (2008).
16. V. P. Tychinsky, "Super-resolution and singularities in phase images," *Phys.-Usp.* **51**, 1205–1214 (2008).
17. N. N. Evtichiev et al., "The laser-aided interference profiler," *Kvantovaya Elektron.* **4**(1), 69–74 (1977).
18. E. A. Andrushtak and V. P. Tychinsky, "The digital phase system for measurement of the parts interference band," *Prib. Tekh. Eksp.* **2**, 169–173 (1980).
19. A. B. Ivanov et al., "The raster method of registering the nanometer-size metabolic activity areas in the phase image of a cell," *Nanotechnol. Russia* **2**(5–6), 54–59 (2007) (in Russian).
20. G. N. Ling, "A new theoretical foundation for the polarized-oriented multilayer theory of cell water and for inanimate systems demonstrating long-range dynamic structuring of water molecules," *Physiol. Chem. Phys. Med. NMR.* **35**, 91–130 (2003). http://www.ncbi.nlm.nih.gov/pubmed/9134752
21. V. Manteifel and T. Karu, "Ultrastructural changes in chondriome of human lymphocytes after irradiation with He-Ne laser: appearance of giant mitochondria," *J. Photochem. Photobiol. B* **38**(1), 25–30 (1997).

Vladimir P. Tychinsky (1925–2014), the prominent expert in basic and applied laser research, is among the pioneers in living cell microscopy. He established the laboratory of coherent phase microscopy and designed the original computer-aided interference microscopes. With these devices the unique properties of phase images, in particular, super-resolution, and cell dynamics became available for analysis. In his last paper he summarized his ideas about general mechanisms that may underlie an astonishing variety of cellular processes.